water

MDPI

Article

Decadal-Scale Variations of Thalweg Morphology and Riffle–Pool Sequences in Response to Flow Regulation in the Lowermost Mississippi River

Chia-Yu Wu * and Joann Mossa

Department of Geography, University of Florida, Gainesville, FL 32611, USA; mossa@ufl.edu
* Correspondence: wuchiayu@ufl.edu

Received: 10 May 2019; Accepted: 3 June 2019; Published: 5 June 2019

Abstract: The lowermost Mississippi River (LMR) is one of the largest deltaic systems in North America and one of the heavily human-manipulated fluvial river systems. Historic hydrographic surveys from the mid-1900s to the early 2010s were used to document the thalweg morphology adjustments, as well as the riffle–pool sequences. Extensive aggradation was observed during 1950s to 1960s, as the Atchafalaya River was enlarging before the completion of the Old River Control Structure (ORCS). Following the completion of the ORCS, reductions in sediment input to the LMR resulted in net degradation of the thalweg profile patterns since the mid-1960s except for the 1992–2004 period. Different flood events that supplied sediment might be the cause of upstream aggradation from 1963–1975 and net aggradation along the entire reach from 1992–2004. Furthermore, the change pattern of thalweg profiles appear to be controlled by backwater effects, as well as the Bonnet Carré spillway opening. Results from riffle–pool sequences reveal that the averaging W_s ratios (length to channel width) are 6–7, similar to numerous previous studies. Temporal variations of the same riffles and pools reveal that aggradation and degradation might be heavily controlled by similar factors to the thalweg variations (i.e., sediment supply, backwater effects). In sum, this study examines decadal-scale geomorphic responses in a low-lying large river system subject to different human interventions, as well as natural flood events. Future management strategies of this and similar river systems should consider recent riverbed changes in dredging, sediment management, and river engineering.

Keywords: thalweg; riffle–pool sequence; lowermost Mississippi River

1. Introduction

1.1. Study Aims

Large alluvial rivers in the world usually have immense socio-economic importance. Different human activities, such as channelization, flood control, or dredging for navigation affected several large drainage systems such as the Nile, Mississippi, Indus, Yangtze, and Euphrates rivers [1,2]. Fluvial geomorphological responses to human impacts are highly dynamic and complex, and the lowermost Mississippi River (LMR) is a notable example (Figure 1). Due to preventing the main channel of Mississippi River from suddenly changing its course (avulsion) into the Atchafalaya River [3], the first phase of the Old River Control Structure (ORCS) was completed in 1963 by the United States Army Corps of Engineers (USACE). After the completion of these structures, different studies discussed whether the ORCS blocked sediments and resulted in sediment deficiency, or stabilized the channel gradient and caused riverbed aggradation [4–16]. In a recent modeling study, Wang and Xu [17] found that, proportionally, more riverbed materials were carried downstream in the Mississippi mainstem

than to the outflow channel. However, they also cautioned that a solid conclusion could not be drawn because the comparison of the modeling results is based on a very limited number of field measurements. Therefore, given the complex morphodynamic behavior in the LMR region, understanding long-term (decadal scale) variations regarding to river thalweg morphology due to anthropogenic disturbance is an important task. With hydrographic data exceeding a century in timespan recorded by the USACE (from the 1870s to 2013), the LMR is an ideal site to study geomorphological response over decadal scales. In addition, the riffle–pool undulation on thalweg profiles is also likely to be indicative of longer-term morphological adjustment and enables an analysis of downstream trends in the riverbed form resistance [18–20].

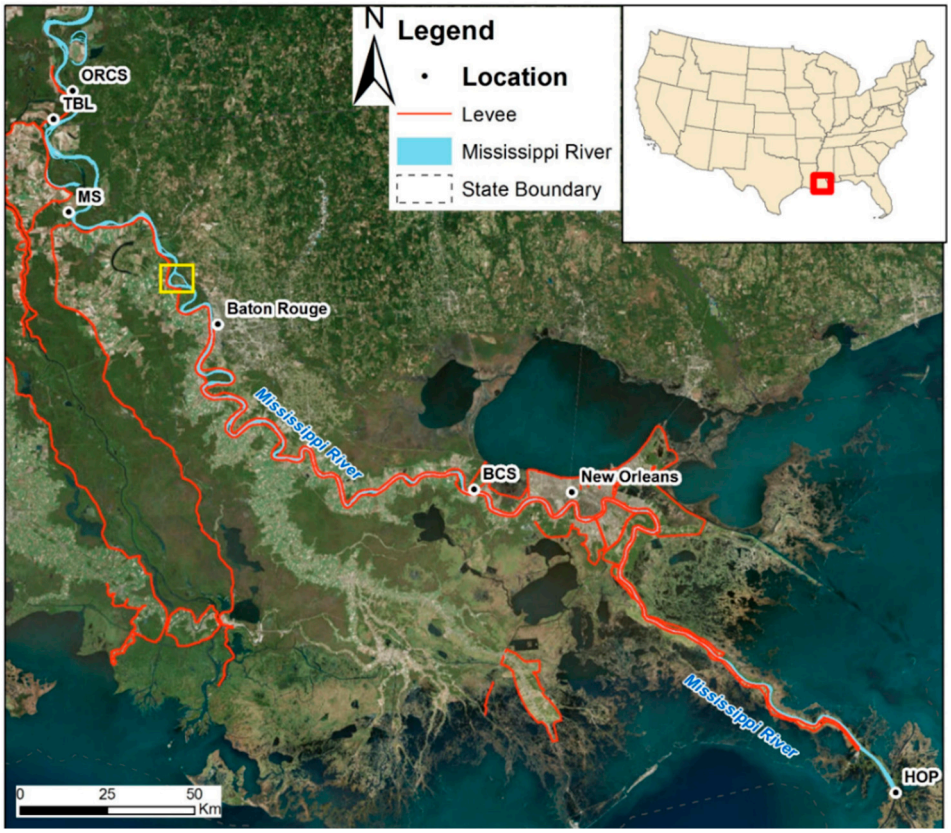

Figure 1. The geographical map of the lowermost Mississippi River (LMR) with different locations. Artificial levees along the channel (red lines) are also marked in this map. Our study reach (river kilometer (RK) 490 to RK 0) is located from downstream of Tarbert Landing (TBL, RK 493) to the Head of Passes (HOP, RK 0). Some important structures are also labeled on the map, such as Old River Control Structure (ORCS, RK 500), Morganza Spillway (MS, near RK 451), and Bonnet Carré spillway (BCS, near RK 205), as well as the two cities of Baton Rouge (RK 370) and New Orleans (RK 164). The yellow square indicates the location for Figure 4B.

Alluvial river channels commonly exhibit a dynamic, three-dimensional variation in the planform, cross-sectional, and longitudinal aspects [21,22]. At the reach scale, the channel thalweg is modified into a series of bathymetric lows and highs. These vertical undulations in bed elevation are generally referred to as riffle–pool sequences. Riffles represent the topographically shallow section of an undulating channel bed, while pools are the topographically deep areas of the channel bed (Figure 2A). The riffle–pool sequences are commonly placed in both straight and meandering rivers with coarse-grained channels of <2% slope [21,23–25]. The morphology of riffle–pool sequences is considered as a fundamental process of channel adjustments in both vertical and planform dimensions [26–30]. Furthermore, riffle–pool morphology is also important in terms of mesoscale habitats, as different physical conditions would determine different habitat type [31,32]. Human activities, such as

channelization or dredging, could modify the riffle–pool forms [33]. Therefore, to examine the variation of the riffle–pool morphology after massive human alterations is another major goal for this study.

In sum, this study aims to examine the variations of thalweg profiles, as well as the riffle–pool sequences, from pre-construction of the ORCS (pre-1963) to recent time (2010s) in the LMR by using the hydrographical datasets. This paper focuses on the lowermost reach of the LMR (Figure 1), extending from the ORCS juncture to the Head of Passes (HOP), which extends from river kilometer (RK) 490 to 0. In general, this study serves as an important extension/comparison to both studies of Joshi and Jun [34], as well as Wang and Xu (see details in Section 1.2). We believe this study will further contribute to understanding of thalweg geomorphology response to a series of engineering interventions in the LMR region over a relatively long-term period (decadal scale).

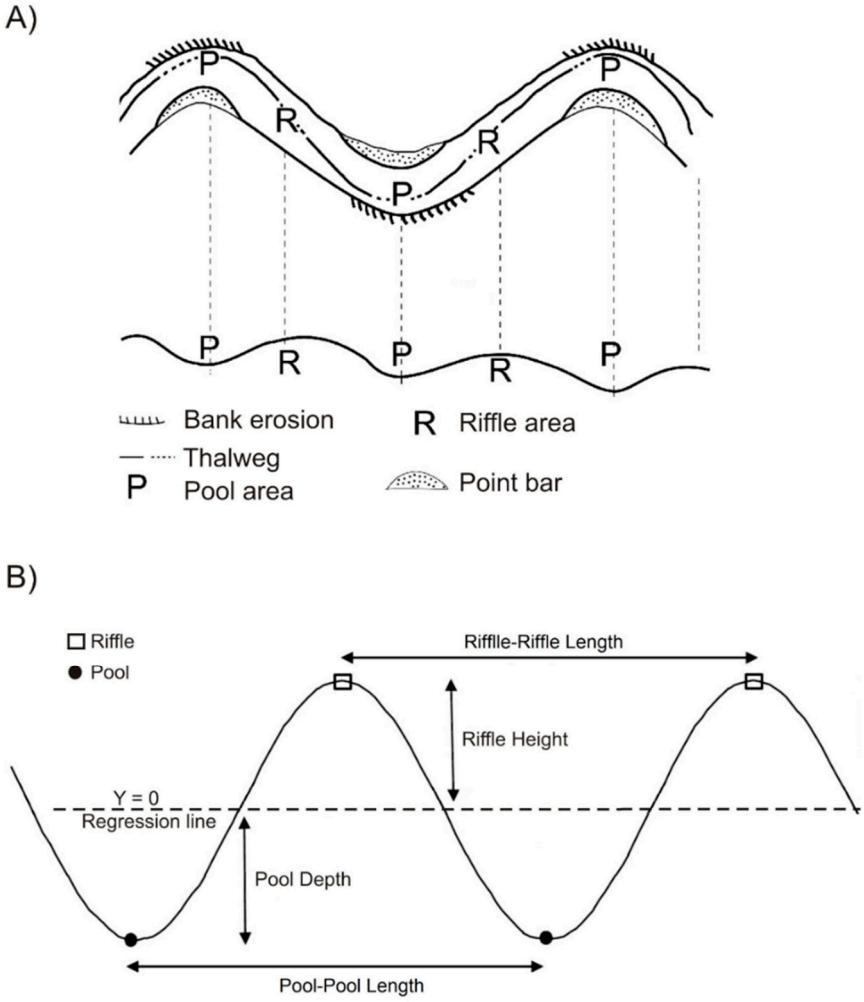

Figure 2. (**A**) The diagram of riffle–pool sequence and planform morphology of a meandering river channel (modified from Keller and Melhorn [27]). (**B**) Definition of bed-form parameters, including the lengths of riffle–riffle or pool–pool, and how the regression line is used to estimate riffle height or pool depth.

1.2. Study Site

The Mississippi River and tributaries drain approximately 41% of the conterminous United States (US); it is also the largest fluvial system around the world. In addition to its role as the largest river in North America, the Mississippi River is a backbone of commerce and industry [4,11,35–38]. The average values of maximum and minimum discharge in Tarbert Landing (TBL) at RK 493 vary from 3143 to 45,845 m^3/s, respectively [14,15]. The drainage area above TBL is estimated to be 2,913,478 km^2.

The LMR is classified as a 10th-order river [39], and the channel bed is composed of latest Pleistocene and Early Holocene fluvio-deltaic sediment [40]. The D_{50} (median particle size) values were reported between 0.05 and 0.28 mm in the LMR, with a gradually finer trend in the downstream direction (Figure 3) [4,37,41,42]. In addition, Keown [41] also indicated that grain size historically became finer from the 1930s to post-1965.

In terms of artificial constructions, since the first artificial levee was erected in New Orleans around the 18th century, the LMR was gradually constrained by different engineering structures such as levees, floodwalls, and revetments [43]. Following the catastrophic flood in 1927, massive upgrades and newly constructed artificial structures were authorized as part of the Mississippi Rivers and Tributaries Project. The history of these engineering interventions was documented by some earlier studies [44–46]. Several outlets and spillways were constructed in the LMR. The spillways and construction times are chronologically as follows: (1) Bonnet Carré Spillway (BCS) near RK 205, completed in 1931; (2) Morganza Spillway (MS) near RK 451, completed in 1954; (3) the ORCS near RK 500, completed in 1963 [47]. The ORCS allows 30% of the combined discharge to pass into the Atchafalaya River, while the other 70% of the total discharge is carried by the LMR [4,48,49]. Despite several other engineering activities after the completion of ORCS [14], it is widely recognized that the LMR is a completely engineered river after the completion of the ORCS in 1963 [49]. However, several studies [4–11] found channel degradation and sediment deficits in the Mississippi deltaic area resulting from dams and other structures (especially the ORCS) trapping vast amounts of sediments upstream within its upper stream. Consequently, there was minimal planform movement of the LMR in the past decades mainly due to confinement by artificial levees, and the protection of these by concrete revetments [5,6].

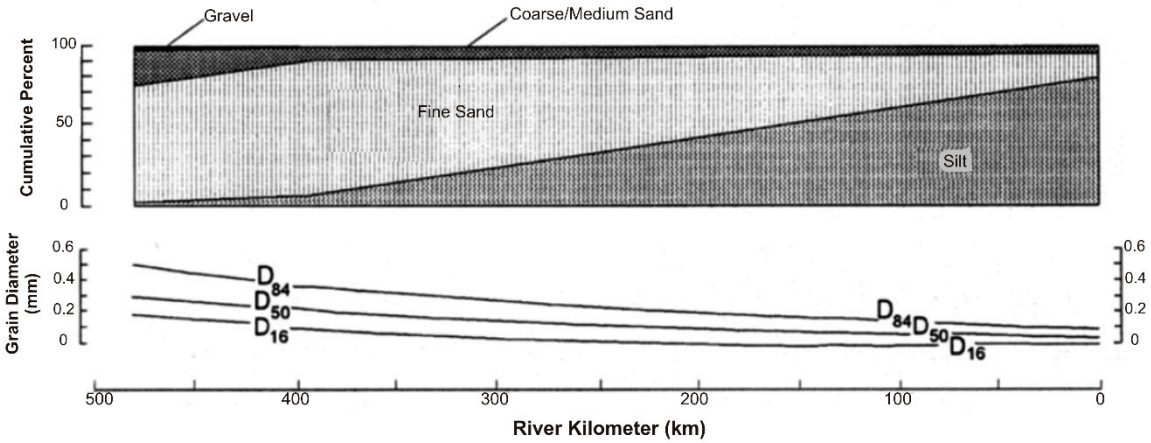

Figure 3. The riverbed materials along the study area (modified from Mossa [4]). The upper graph shows downstream changes in bed material using different terms (i.e., gravel, sand, silt, clay), and the lower graph shows grain size in numbers (i.e., D_{50} is the median grain size, while D_{84} and D_{16} are the 84th and 16th percentiles used to represent the coarse fraction, respectively).

Contrasting these other studies, Joshi and Jun [34] analyzed the riverbed adjustment by using 18 cross-sections near gauging stations, as well as river stage data, from 1992–2013. They found the channel degradation was only observed in a 60-km reach (out of 500 km in total), whereas all the other reaches were either experiencing gradual aggradation, or showed no significant change over time. They concluded that, since the LMR generally received less flow than it did beforehand due to ORCS regulation, there were lower water velocities, which could further benefit in sediment deposition along the reach. Similar observations with sediment deposition in the LMR were also observed by Biedenharn et al. [50], as well as Wang and Xu [14]. Biedenharn et al. [50] analyzed the stage and discharge data from gauging stations from 1880–1992 and summarized that the river in the post-cutoff period (1943–1992) had a much greater stream power than in the pre-cutoff (1880s–1930s).

Furthermore, Wang and Xu [14] utilized the hydrographic survey data from 1992–2013 and identified both degrading and aggrading sub-reaches; nevertheless, this study also indicated that a vast amount of sediment was deposited in the LMR channel, especially between RK 386 and 163. Note that one important aim of this study is to extend and compare the study period from Wang and Xu [14] and Joshi and Jun [34]. As both these studies merely focused on the period from the 1980s to the 2010s, our study covers from the 1950s to present. Therefore, we believe this study will give a broader view from past to present on the channel dynamics of the LMR.

1.3. Previous Studies on Riffle–Pool Sequence

The morphological characteristics and controlling variables of riffles and pools were intensively investigated in different aspects, such as meander wavelength or channel width [24,28,30,51,52], flow velocity or energy [24,30,51,52], and sedimentation processes [53–56]. In addition, the maintenance of the pool–riffle form was also discussed in several studies [57–59], such as the role of obstructions in the pool, sediment routing around the pool, and sediment structure differences between pools and riffles. Although some arguments remain regarding the initiation and maintenance of riffle–pool sequences, such as velocity (or shear stress) reversal hypothesis [55,60], several observations in common are supported by numerous studies. One of these observations is the spacing between pools or riffles being roughly 5–7 times the channel width (denoted as the W_s ratio, Figure 2B). Furthermore, since the meander wavelengths usually consist of two riffle–pool sequences, the meander wavelengths should be 10–14 times the channel width [27,28,53,61–65].

Despite over 100 scientific papers discussing the pool–riffle sequence, most of these studies examined the variations of riffle–pool sequences within small channel systems or mountainous rivers [64,66,67]. Only few studies focused on highly engineered large river systems, especially for long-term observations [19,22,33,68]. The lack of studies focusing on the riffle–pool sequence in these river systems can be summarized as being due to two different reasons. Firstly, erosion and sedimentation rates in large alluvial floodplains are often various and complex to estimate. Secondly, the study of riffle–pool morphology usually requires detailed field surveys, which is particularly difficult in large river systems [22,69].

Keller [33] was the first to discuss whether the development of riffle–pool sequences could be affected by the variety of stream conditions, especially between natural and channelized streams. Keller's [33] pioneering study only examined small portions of six rivers (<1 km) without discussing the possible thalweg changes over time. On the other hand, Dury [68] used long-term monitoring data (approximately 100 years) to investigate the changes in riffles and pools in Hawkesbury River, Australia. Our study also utilizes long-term (>50 years) decadal-resolution data to examine the variations of thalweg profiles, as well as the riffle–pool sequences from a period of moderate human impact (before the completion of ORCS) to a period of heavy human impact (post-ORCS construction in 1963).

1.4. Relevant Studies in the LMR

Numerous prior studies summarized different aspects of human modifications of the LMR, such as sedimentation deficit [5–8,38,70] or geomorphological or hydrodynamic responses to human impact [50,70–73]. Only few studies [19,22,65,69] aimed to investigate the temporal and spatial variations of the thalweg profiles and riffle–pool sequences. Among these studies, Hudson [22] was the first to discuss pool–riffle morphology in the LMR. This study aimed to investigate the pool–riffle morphology changes before massive engineering modification. Therefore, their study area was upstream (from Cairo, Illinois to approximately the TBL) from the 1880s to 1910s. Therefore, their study area and period do not overlap with our study.

Harmar et al. [19] was another notable research that analyzed riffle–pool sequences and morphological adjustments by using hydrographic surveys from RK 1017–574 (between the confluence of the Arkansas River and 8 km upstream from ORCS) from 1949–1989. They suggested that the greatest changes occurred during the post cut-off period (1949–64) upstream from Vicksburg, Mississippi.

However, this study used cross-sectional data from prior to the 1990s, and the morphological adjustments or sedimentation rates in the LMR might have varied after different modern flood events, such as the 1993 or 2011 floods [74–76]. Furthermore, similar to Hudson [22], this study also did not overlap with our study area. Note that, although Gibson et al. [65] also studied riffle–pool sequences in the LMR, their study solely used 2013 hydrographic survey to identify pools in the LMR. In sum, our study is a pioneering and unique attempt to document all the hydrographic surveys from the late 1940s to early 2013s. This study may further help understand how the lowermost Mississippi river adjusted to increasing engineering and human modification.

2. Materials and Methods

2.1. Constructing Thalweg Profiles

The hydrographic surveys collected by USACE along the LMR comprise across-channel sounding points with elevations [19]. These hydrological surveys are repeated roughly each decade, which not only contribute insights into the thalwag changes at decadal intervals, but also enable a more rigorous analysis of morphological changes than previously possible. These cross-sections are longitudinally spaced at 250–400-m intervals along the entire LMR, with 15–50 sounding points per cross-section; the number of sounding points depends on channel width. These sounding points were spaced at 30–40-m intervals along each cross-section. With sufficient spatial and temporal resolution, several previous studies utilized these datasets for their research [6,14,19,22,34,37,69,77,78]. In our study, these hydrographic transects were employed to construct the thalweg profiles for six different times, including 1952, 1963, 1975, 1992, 2004, and 2013. All the hydrographic data share the same horizontal coordinate system (i.e., State Plane system, Louisiana south). Table 1 summarizes all the hydrographic surveys and their characteristics.

Table 1. Summary of different hydrographic surveys used in this study.

Name Adopted in the Article	Dates of Survey	Number of Maps in Series	Cross-Section Numbers Used
1952	1949–1952	80	1892
1963	1961–1963	86	1829
1975	1973–1975	86	1831
1992	1991–1992	86	1831
2004	2003–2004	104	1832
2013	2013	86	1832

In order to construct profiles of thalweg elevation, we delineated the lowest elevation point in each cross-section from the hydrographic survey sheets (Figure 4A). A series of shapefiles were generated in different years by digitizing all the thalweg points in the respective hydrographic survey. Furthermore, the channel width was measured as the distance between two bankfull lines (Figure 4A). With channel width in each riffle or pool, we could further estimate the widths in riffles or pools, and calculate different ratios (e.g., W_s, see details in next section). Note that all the elevation data were utilized in our analysis, except the data covering a 5-km-long chute at Profit Island near RK 400 (the cross-sections in yellow of Figure 4B).

To allow direct comparison between hydrographic surveys, each cross-section was referenced to a normalized channel distance, based on the river miles (RM) above HOP measured by USACE in 1962; all the RM were converted to RK afterward. Note that we averaged thalweg depths every 1000 m to create the thalweg profiles for temporal comparisons, which also allowed our results to compare with Hudson and Kesel [69]. Furthermore, the elevation soundings during 2004 and 2013 were vertically referenced to the North American Vertical Datum of 1988 (NAVD 88), while other elevation soundings in all the older hydrographic surveys were based on the National Geodetic Vertical Datum of 1929 (NGVD 29). For consistency, these survey data were converted to NAVD 88 using the CORPSCON

program developed by USACE [79]. In addition to the hydrographic survey data, daily discharge recorded at TBL by USACE was also employed to characterize hydrological changes from 1949 to 2013.

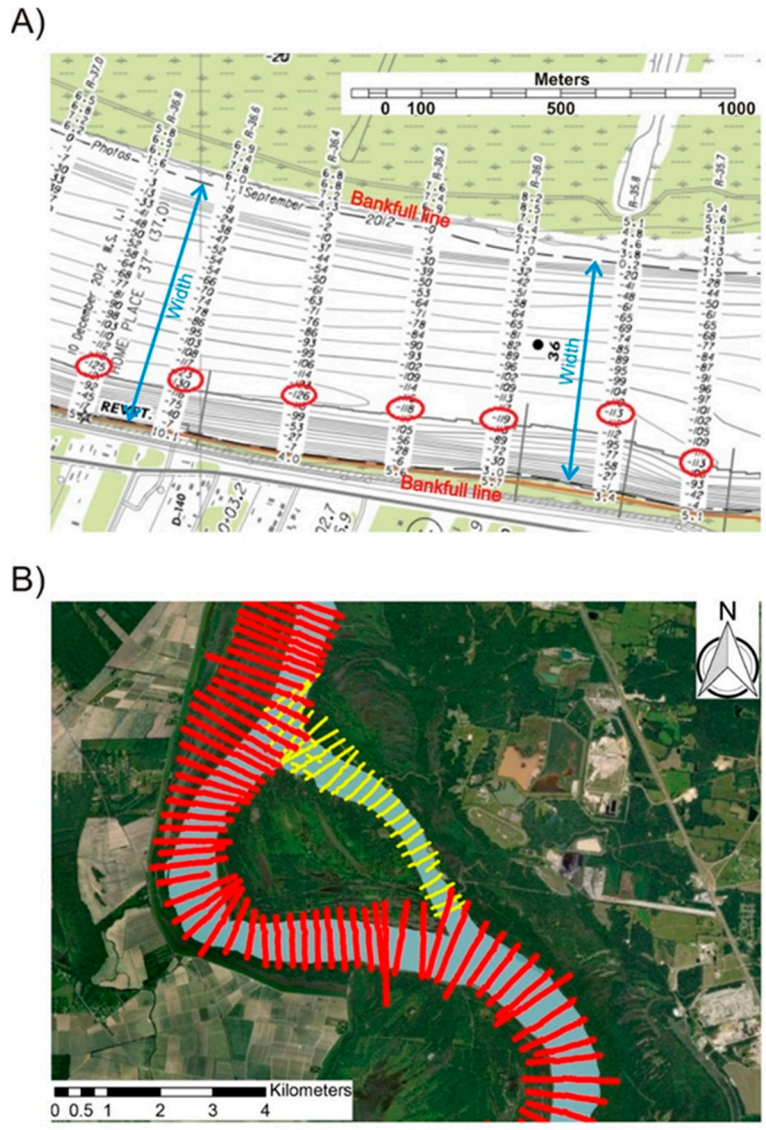

Figure 4. (**A**) The diagram from the hydrographic survey in 2013 shows the schematics of how the channel width (blue lines with arrows) and thalweg points (red circles) are determined. The bankfull or water surface lines are marked by the United States Army Corps of Engineers (USACE), and the channel width is defined by the distance between two bankfull lines. (**B**) The map shows a sand bar dividing the cross-sectional survey in 2013. Those cross-sections in red were located in the main channel and, therefore, were kept in our study, whereas the cross-section in yellow was deleted from our study. See the location in Figure 1.

2.2. *Riffle–Pool Identification and Analysis*

Carling and Orr [80] reviewed over 50 studies and concluded that there are only four robust, objective analytical techniques to identify riffle–pool sequence (Table 2), and most of the studies adopted one of these principal techniques. Among all the identification techniques, the "bed-form differencing technique" developed by O'Neill and Abrahams [81] is the most common method that was employed by several studies [19,22,64,65,82]. This method, therefore, was employed in our study. O'Neill and Abrahams [81] addressed that the topographic high or low would be identified as a riffle or a pool once the cumulative bed-form elevation exceeds the tolerance value (T). In this

study, T of 6 m was selected based on the results from Harmar et al. [19], as well as Harmar [83], as both studies performed sensitivity analyses by employing similar hydrographic surveys to this study. Note that riffles and pools were identified by using the constructed thalweg profiles from 1952, 1963, 1992, and 2013. Delineating the riffles and pools between 1952 and 1963 typifies the changes of riffle–pool sequences prior to completion of the controlled diversion at ORCS with less engineering, whereas post-1963 riffle–pool sequences feature the patterns with controlled diversion and increased engineering structures such as revetments. In addition, using 250–400-m gaps between two intermediate cross-sections might sometimes result in not capturing pools or riffles. However, several studies [19,22,65,83] employed these hydrographic transects, and suggested that these data provide sufficient resolution for the identification of riffles and pools.

Table 2. Different methods for analyzing riffle–pool sequences.

Method	Description	Studies Advocating This Method
Zero-crossing analysis	Fitting a regression model for the bed profiles to identify positive (riffle) and negative (pool) residuals departures from zero (regression line).	[28,68,84]
Bed-form differencing technique	This method identifies pools and riffles by checking if cumulative elevation changes exceed a certain tolerance value. The tolerance value is usually based on the standard deviation of successive differences in bed elevations.	[81]
Power spectral analysis	Similar to spectral analysis, describing thalweg data as both periodic and random fluctuations. A second-order recreation is used for autoregressive process.	[29]
Control-point method	Extending the base flow water surface upstream from the low point in each riffle crest until it intersects the bed upstream; then, the pool lengths can be defined.	[51]

Once all the riffles and pools were identified, different features of riffle and pool morphology could be measured, such as channel width, amplitude of each riffle or pool (riffle height or pool depth, and the length (or spacing) between two consecutive pools or riffles (Figure 2). The length of each bed-form is the distance between a pool and the other downstream pool, or riffle and the other downstream riffle (Figure 2A). Furthermore, the amplitude of each sequence was decided with the maximum deviation beneath (pool) or above (riffle) the regression line (Y = 0 regression line in Figure 2B). With the results of amplitude and length, different ratios, such as W_s or W/D (width-to-depth ratio), could be estimated. The entire procedures were performed using SPSS, Python code, and ArcGIS. Note that the entire LMR was divided into the upper and lower reaches at the BCS (Figure 1). The reason for employing this break point is outlined in next section.

3. Results

3.1. Thalweg Profiles

Figures 5 and 6 display six different hydrographic surveys profiles from 1952 to 2013. Four profiles identified pools and riffles (Figure 5A–D). All these thalweg profiles exhibit a general declining trend toward the downstream direction that reverses approaching the HOP. All the thalweg profiles show periodic oscillations in the downstream direction, which are mainly regulated by well-developed riffle–pool sequences; however, the thalweg profiles in the last 30-km reach (RK 30 to HOP) rise sharply by about 20 m. Because the riffles and pools become more difficult to identify due to their decreased amplitude, all the identified riffles and pools are located upstream of RK 30.

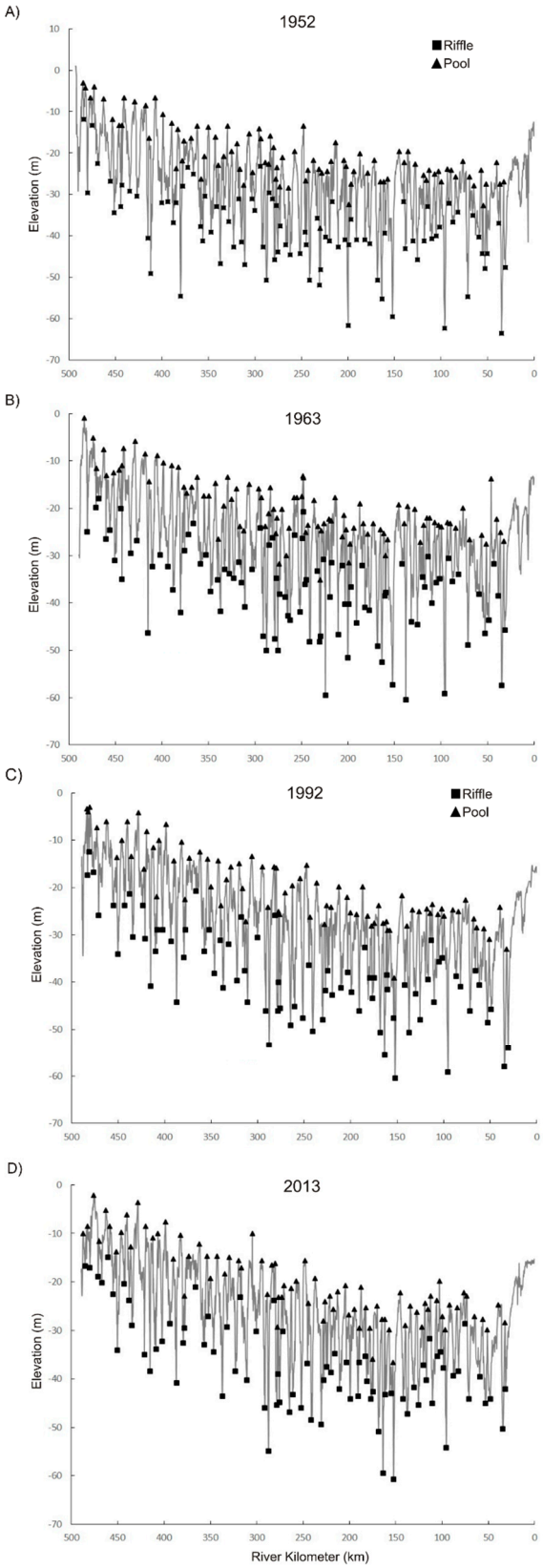

Figure 5. The long thalweg profiles with identified pools and riffles for four hydrographic surveys in 1952 (**A**), 1963 (**B**), 1992 (**C**), and 2013 (**D**). Each thalweg profile is referenced to a standard channel distance from RK 490 to HOP at RK 0. The elevation values are above the North American Vertical Datum of 1988 (NAVD 88).

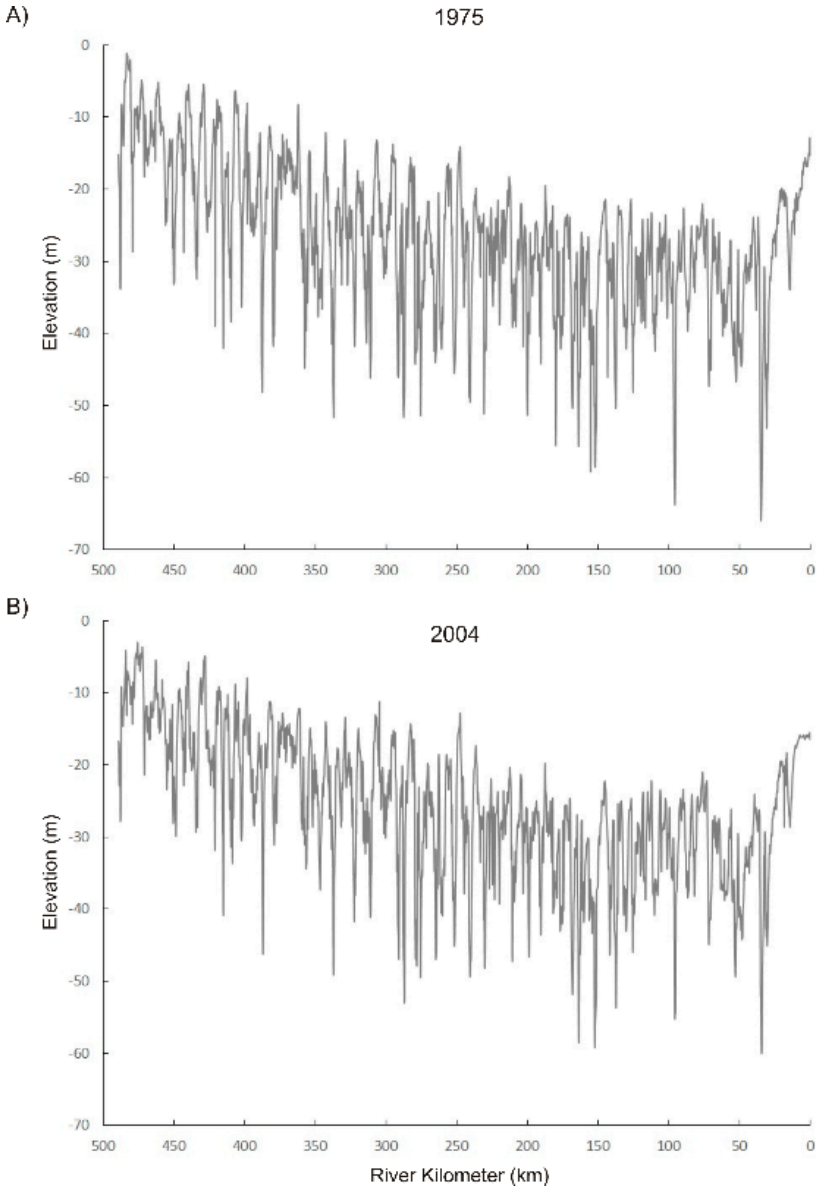

Figure 6. Two other thalweg profiles in 1975 (**A**) and 2004 (**B**) are only used for comparing the cumulative elevation changes of thalweg in different times without identified riffles or pools. The elevation values are above NAVD 88.

A comparison of downstream variations in thalweg elevation between the two endpoints (1952 and 2013 profiles) are displayed in Figure 7. A linear regression line was employed on the profile of Figure 7A, with an estimated slope coefficient of −0.008 (see formula in Figure 7A). This slope coefficient represents the overall elevation change of 8 cm for every 10 km in the downstream direction. Over the 65-year duration, the characteristics of the thalweg elevation change demonstrate that most of the riverbed experienced channel aggradation (i.e., most of the *y*-axis values >0 on Figure 7A). However, the trend in Figure 7A does not reveal where and when the highest rates of degradation occurred. Therefore, a cumulative elevation change (Figure 7B) was generated for further comparison.

The trend in Figure 7B reveals a clear difference between upstream and downstream of the BCS (RK 205). A constant increasing trend upstream of the BCS indicates consistent aggradation rate throughout this reach. Meanwhile, there is no constant trend downstream BCS, with a decreasing trend (RK 205–125), which relatively flattened (RK 125–30), before increasing to HOP (RK 30–0). Following these observations, it would be more appropriate to examine thalweg profiles by employing two

different reaches (upstream and downstream BCS), rather than one. Hence, two major reaches were divided in this study: upper (RK 500 to RK 205) and lower (RK 205–0).

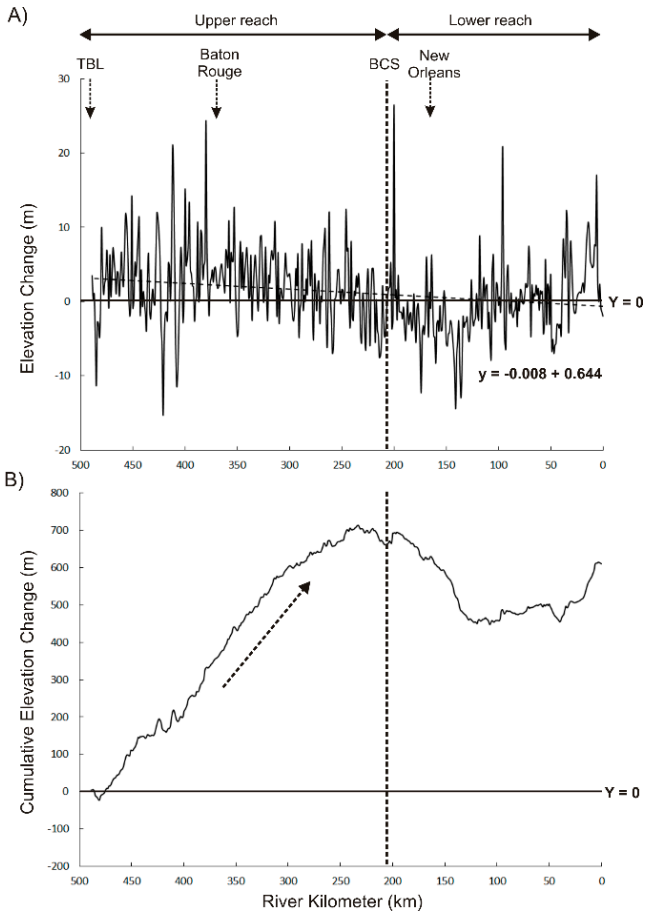

Figure 7. Changes to the thalweg profiles between 1952 and 2013 in the LMR: (**A**) linear regression (dashed line) of elevation change; (**B**) cumulative elevation change, where the dashed line with an arrow represents a constant aggradation trend. Different locations are also labeled to represent the relative position. Note that location of the BCS (labeled as a dashed line) serves as the break point of the upper and lower reaches in our study.

3.2. Cumulative Elevation Changes

The cumulative elevation changes were generated using all the intermediate hydrographic surveys from 1952 to 2013 (Figure 8). Notable changes in both the upper and lower reaches in different time periods can be found from Figure 8. From 1952–1963, before the completion of ORCS, the general trend increased with a relatively flat span around RK 205 to RK 120, which implies a consistent aggradation along the entire study reach. The trend line from 1963–1975 (orange line in Figure 8) shows a different pattern than that from 1952–1963. Although local aggradation occurred in the reach upstream of RK 360, it was less than the earlier period with minimal change (flat) between RK 360 and 205, whereas the lowermost reach (downstream RK 205) experienced pronounced degradation. Therefore, the phenomenon of net sediment erosion can be found just following completion of the ORCS in 1963.

Both the trend lines after 1975 (1975–1992 and 2004–2013) also show a net degradation patterns (blue and purple dashed lines in Figure 8). Specifically, although local aggradation occurred in the trend line of 1975–1992 (RK 360–265), the general trend still reveals net degradation in both periods. The only exception is the trend line of the 1992–2004 period; the red line in Figure 8 shows net aggradation during this period, which is similar to the trend line in 1952–1963, but the cumulative change is considerably less. In general, the vertical adjustments (aggradation, degradation, or no notable change) between

1952 and 2013 are summarized in Table 3. A prominent finding, similar to the observation previously discussed, is that the BCS also appears to be a change point between the upper and lower reaches.

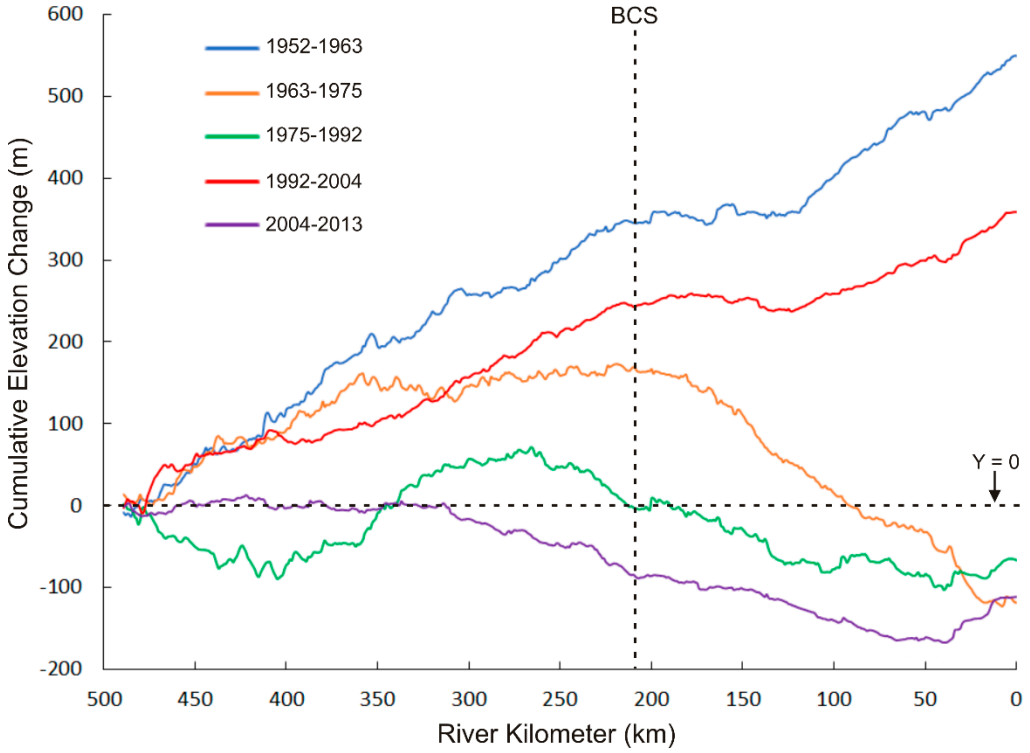

Figure 8. The cumulative elevation changes with the upper reach and lower reach (divided by the BCS) shown by intermediate hydrographic surveys from 1952 to 2013. A positive trend represents sediment deposited on the riverbed, while a negative trend indicates sediment erosion in the study area.

Table 3. Vertical trends (degradation, aggradation, or no change) in thalweg profiles during different periods from 1952 to 2013 (See Figure 8). The numbers in this table represent distance in river kilometers (RK; i.e., 205–120 indicates the sub-reach from RK 205–RK 120).

Period	Degradation	Aggradation	Slight/No Change
1952–1963	–	490–205, 120–0	205–120
1963–1975	205–0	490–360, 40–0	360–205
1975–1992	270–0	360–270	490–360
1992–2004	–	490–205, 120–0	205–120
2004–2013	310–40	40–0	490–310

3.3. Riffle–Pool Amplitude, Length, and W_s Ratio

Most of the previous studies reported that lengths of pool–pool or riffle–riffle should be 5–7 times the channel width (W_s ratio). Although the greatest number of pools and riffles is not always spaced from 5–7 channel widths apart (most of the values concentrate from 3–5), the average numbers still fall in this range (with the only exception for the riffle average value in 1992 = 8.06) (Figure 9). These patterns are consistent with previous studies [27,28,53,61–63].

The statistics of spacing (e.g., pool–pool length and riffle–riffle length), pool depths, and riffle heights in both upper and lower reaches are summarized in the length values of Table 4. It is observed that the results of the lengths (both pool–pool and riffle–riffle) in both upper and lower reaches nearly overlap with each other (see Figure S1, Supplementary Materials). The riffle heights are displayed in the amplitude values from Table 4; the results show relatively stable from 1952–2013 for both upper and lower reaches, where the values range from 6.7–7.9 m. Nevertheless, the average pool depths fluctuate from 9.1–12.0 m, greater than the average riffle heights.

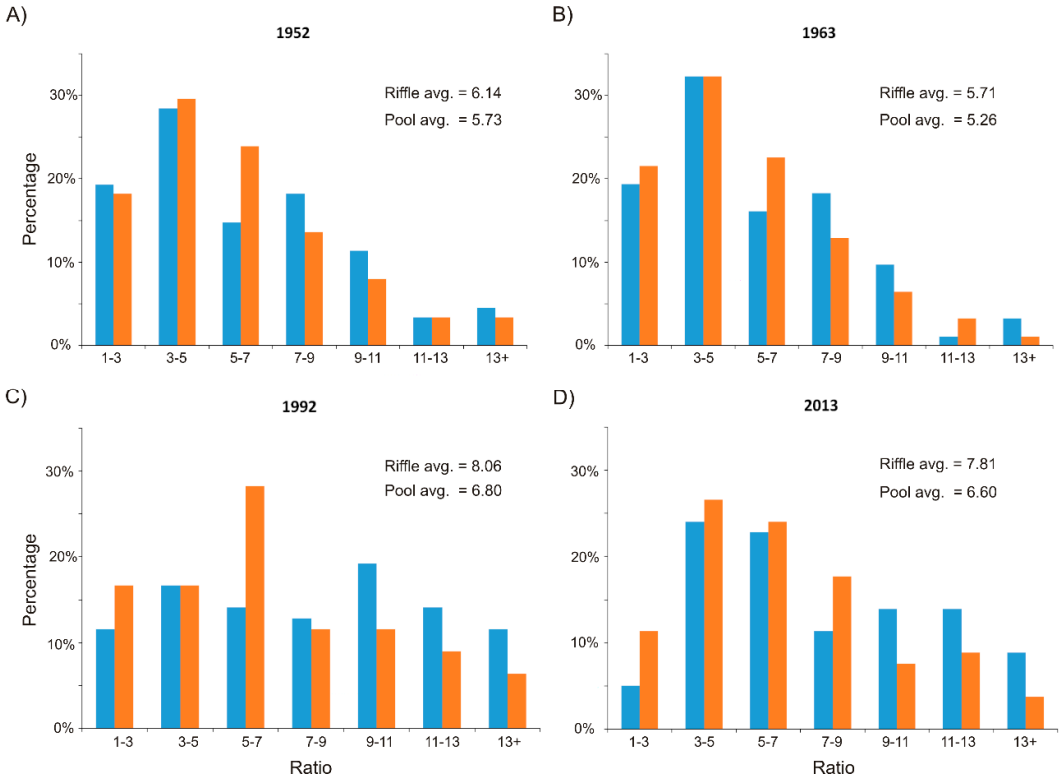

Figure 9. Frequency of pool–pool length (in orange) and riffle–riffle length (in blue) by channel widths (W/D ratio) at different times: 1952 (**A**), 1963 (**B**), 1992 (**C**), 2013 (**D**). Averaged W/D ratios of riffles or pools are also displayed in this figure.

Table 4. The average values of the length (i.e., the length between two consecutive pools or riffles), amplitude (i.e., riffle height, pool depth), and W/D ratio (width-to-depth ratio) for riffles and pools in different survey years. These average values are displayed by riffles in the upper reach (UR) and lower reach (LR), as well as pools in the upper reach (UP) and lower reach (LP). The values in both length and amplitude represent distances in meters.

	Year	UR	UP	LR	LP
Length (m)	2013	6099	6099	5220	5209
	1992	5890	5918	5534	5563
	1963	4781	4728	5056	5046
	1952	4932	4972	5373	5389
Amplitude (m)	2013	6.67	11.33	6.97	9.11
	1992	6.84	11.99	7.04	10.66
	1963	7.25	9.86	7.89	10.17
	1952	7.41	10.89	7.59	11.15
W/D ratio	2013	141.00	70.10	107.86	78.71
	1992	136.93	68.38	103.42	65.80
	1963	130.99	88.96	104.92	76.31
	1952	125.94	82.64	106.60	69.48

4. Discussion

4.1. Cumulative Elevation Changes

Based on the patterns in Figure 8, net aggradation occurred from 1952–1963, before the completion of the ORCS; this finding is different from the results of Hudson and Kesel [69] or Harmar et al. upstream [19]. Both studies concluded that, following massive construction of artificial cut-offs and reservoirs, the degradation rates were high during the same time span (1952–1963). Note that both of these studies [19,69] examined the river upstream of the ORCS, whereas our study scrutinizes the LMR further downstream. Perhaps some of the bed sediment which eroded upstream during this period was transported into the reach downstream, resulting in net deposition in our study area.

It is widely recognized that the completion of the ORCS changed the flow and sediment regime of the system [4,6,7,9,85]. What is uncertain is whether the structure could cause the entire LMR to shift from aggradation to degradation. As a result, net degradation occurring after 1963 is expected. Therefore, Figure 8 reveals that, despite some local aggradation, the trend lines of 1963–1975, 1975–1992, and 2004–2013 share a similar net degradation pattern. Upstream degradation (RK 490–360) from 1963–1975 might have been affected by the 1973 flood, as both in channel and overbank sediments deposition were found near the ORCS [86]. Furthermore, the disparity between the 1952–1963 trend line and the dashed line (Y = 0 line in Figure 8) gradually increases in a downstream direction. Nevertheless, although net degradation occurred in the LMR after 1963 (except for the 1992–2004 period), the scales of disparity (between post-ORCS trend lines and Y = 0 dashed line) are relatively small. Therefore, the thalweg profiles seemed to gradually reach an equilibrium state after the ORCS completion.

As mentioned above, the trend line in 1992–2004 is the only time period with net aggradation after the completion of the ORCS in 1963. One possible reason for net aggradation might be due to the 1993 flood. Several studies [12,14,37,87] reported that discharge over 2.5–2.6 $\times$ 10^4 m^3/s would trigger channel erosion in the LMR. On the contrary, they also suggested that, if discharge was less than this threshold value (i.e., 1.8–2.5 $\times$ 10^4 m^3/s), it would cause channel aggradation. Figure 10 displays both the peak discharge and duration (days) at TBL by applying the previous criteria. The duration of deposition tendency during the 1993 flood (185 days) is prominently longer than any other years (orange histogram in Figure 10). Therefore, one possibility is that the 1993 flood may have contributed to vast amounts of sediment deposition [14]. However, in contrast, using data from instantaneous discharge measurements with higher temporal resolution from TBL (RK 493), manipulated as in Mossa [88], suggests that bed changes at this location were minimal when comparing before and after the 1993 flood with thalweg elevation rising and falling by ~3 m during the year (Figure 11). Unfortunately, these data only exist for selected locations with frequent discharge measurements; thus, it is not possible to examine other locations with this degree of detail.

In addition, the functioning of the BCS might also explain downstream aggradation from1992–2004. The BCS is designed to divert flood discharge from the main Mississippi River into Lake Pontchartrain, in order to ensure that the discharge flowing through New Orleans is less than 3.5 $\times$ 10^4 m^3/s. Until the 2011 flood event, the BCS was opened 10 times since its completion during 1931 [42,89], with eight of the 10 instances occurring during our study period (Table 5). As the water surface recedes during floods near this location, the drawdown effect might decelerate the sediment deposition in the downstream reach and flatten the trend lines, especially from 1952–1963 and 1992–2004 (RK 205–120 in Figure 8 and Table 3). Note that the BCS was not opened during the 1993 flood (Table 5); therefore, none of the sediments coming from upstream would have an opportunity to exit the river and, thus, would either be deposited upstream or downstream of this reach. Given all the previous explanations, the pattern of channel aggradation from 1992–2004 is reasonable and has several possible explanations [14].

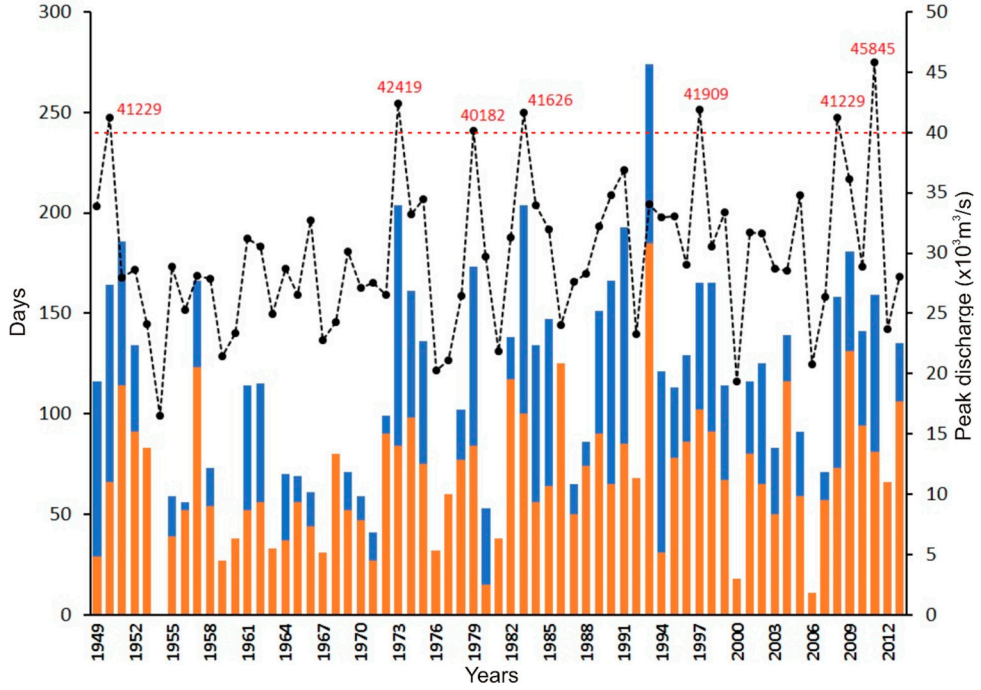

Figure 10. The peak discharges (black line with dots) at TBL from 1949 to 2013. The BCS was opened during every flood event except the 1993 flood [89] (see Table 5). In contrast, the duration of discharge from 18,000–32,000 m^3/s is also marked on the histogram. Peak discharges during seven flood events above the red dashed line (40,000 m^3/s) are marked with a red number. The duration in days of discharge from 18,000–25,000 m^3/s (orange color, tending to deposition) and above 25,000 m^3/s (blue color, tending to erosion) are also marked on the histogram. It is observed that the longest period (185 days) of deposition occurred during the 1993 flood, whereas the longest erosion duration (120 days) took place during the 1973 flood.

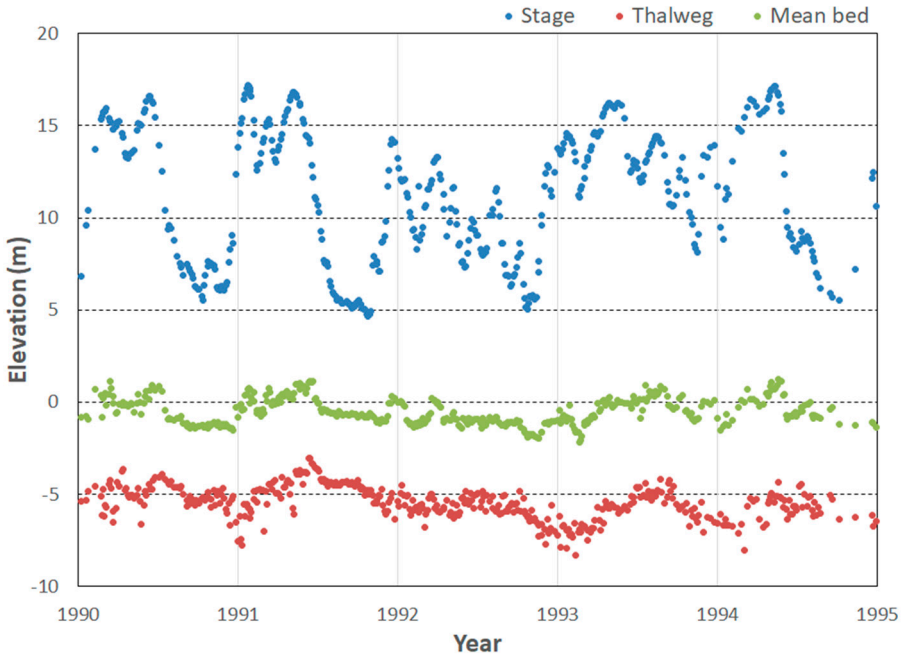

Figure 11. The stage (blue), mean bed (green), and thalweg (red) elevations at TBL from 1990 to 1995 manipulated from data collected by the USACE. Although high stages could be found during the 1993 flood, and ~3 m fluctuations in both mean bed and thalweg elevations occurred, this site had no net aggradation.

Table 5. Opening dates of the Bonnet Carré Spillway (BCS) due to different flood events from 1950 to 2011. This table also includes maximum bays open, maximum water discharge, and estimated sediment deposition (modified from Day et al. [89]).

Year †	Dates Spillway Opened	Max. Number of Bays Open	Max. Discharge (m^3/s)	Sediment Deposition ($10^6 \times m^3$)
1950	February 10–March 19	350	6315	3.8
1973	April 8–June 21	350	5523	11.5
1975	April 14–26	225	3115	1.5
1979	April 17–May 31	350	6457	3.8
1983	May 20–June 23	350	7590	3.8
1997	March 17–April 18	298	6797	6.9
2008	April 11–May 8	160	4531	1.5
2011	May 9–June 20	330	8949	7.2

† This table excludes the 1994 opening, which was for experimental purposes, not for flood control.

If we neglect the trend lines that were affected by the flood events (i.e., trend line from 1992–2004, RK 490–360 in the 1975–1992 trend line), all the trends in Figure 8 post-ORCS (after 1963) show a relatively similar pattern, i.e., no change or aggradation upstream of the BCS (RK 205), while showing degradation in the lower portion (RK 250–40). This thalweg deformation pattern may result from backwater effects [14,37,87,90]. Backwater effects usually occur within the backwater zone; in the Mississippi River, the backwater zone extends from the HOP to RK 650 [42]. Backwater effects take place when a river approaches its outlet, where the flow decelerates because of lateral spreading and vertical deepening in the channel [91,92]. Several models demonstrate that the lower part of the LMR (last 150-km reach) may experience erosion, but deposition in the upper part [42,87,90]. Another related explanation is that the LMR is tidally influenced and the salt-water wedge moves further upstream during low water, such that an underwater sill needed to be constructed near RK 102 on the bed of the river to guard the water supply at New Orleans during drought [93,94]. Moving toward the mouth, bi-directional tides may mute out riverine processes and related forms, resulting in far more subdued bed-forms.

Finally, thalweg aggradation occurred in the last 40-km reach (Figure 8), except for the 1963–1975 period; different studies [14,37] also reported similar observations. The high deposition rate might be triggered by different factors, such as accelerating sea level rise in the recent decades [95], as well as natural crevasses and river passes [14], resulting in the reduction of flow velocity in this reach. In addition, salt-water wedge intrusion also causes seasonal sediment deposition in the estuary [96]. Nevertheless, channel degradation that occurred sometime from 1963–1975 might also have resulted from the 1973 flood. Within roughly 3–3.5 $\times 10^4$ m^3/s of daily discharge passing through New Orleans (downstream BCS) during this flood event [97], Chatanantavet et al. [87] suggested a strong erosion tendency near the LMR estuary. Therefore, it is reasonable to observe the degradation from 1963–1975 in this reach.

4.2. Statistical Results of Riffles and Pools

The distribution of W_s ratio (Figure 9) shares similar patterns to several other studies [27,33,84]; as their histograms also depicted that the greatest percentage of the W_s ratio fell within a range of 3–5, although average values fell within 5–7. Both Hudson [22] and Gibson et al. [65] reported average W_s ratios of around 7 by examining the thalweg data at RK 1618– 483 [22] or RK 490–0 [65]; these results are consistent with our results. In general, the W_s results from this study are coherent with most of the previous studies. Nevertheless, averaged pool depths reported by Gibson et al. [65] were higher (16.4 m) than the similar results from this study (9.1–12.0 m; see the amplitude values in Table 4). Note that Gibson et al. [65] measured the pool depths by directly using the difference between the deepest pool point and the highest point of the adjacent riffle. Therefore, by combining the mean riffle

heights and pool depths in our results (the amplitude values in Table 4), our results also ranged around 16.1–18.9 m, consistent with the amplitude measurements reported by Gibson et al. [65].

The shortest length of both pool–pool and riffle–riffle occurred in 1963, while both longest lengths were found in 1992 (the length values in upper part of Table 4). Small-scale oscillations were measured for both lengths and pool depths, but the riffle heights were stable. The pattern change may suggest that the configuration of riffle–pool sequences adjusts due to flood events during the time intervals [19]. In the upper reach, the greater pool length value appeared in both 1992 and 2013, together with the smaller pool depth value occurring at the same time (middle part in Table 4). Similar findings were reported by Harmar et al. [19] upstream; their study suggested that the greater values of amplitude and length (for both riffle and pool) in 1975 might have resulted from the 1973 flood (Figure 10). They proposed that, to exhaust additional energy during a short period of extreme high flow, the riverbed tends to adjust its morphology to enhance bed-form resistance. This model might explain our findings, as the 2013 results may reflect the bed-form adjustments resulting from the 2011 or 2008 flood events. Correspondingly, the outcomes from 1992 might have resulted from the 1983 flood.

4.3. Cross-Sectional and Temporal Adjustments of Riffle–Pool Sequences

The results from W/D (width-to-depth ratio) can indicate the form resistance of cross-sectional geometry, which depend on the characteristics of the sediment material or bankfull confinement [19,22,24,28,98]. The W/D results are displayed in Figure 12 (upper reach) and Figure 13 (lower reach), as well as W/D ratios in Table 4. There are two important discoveries revealed by Figures 12 and 13; firstly, the W/D ratios display a clear difference between riffles and pools. The dashed line of 50 W/D roughly divides riffles (usually with a larger ratio) from pools (usually with a smaller ratio). This division is expected because riffles are known to be both wider and shallower morphological features, thereby providing a greater form resistance than pools [19,28]. Secondly, the average W/D ratios (Table 4) decrease from the upper reach (W/D ratio for riffles = 134, and for pools = 78) to the lower reach (W/D ratio for riffles = 106, and for pools = 73). A potential reason for the variations of W/D ratios may be due to the characteristics of the riverbed sediments. Figure 3 shows the decreasing trends of bed material size in the downstream direction mentioned previously (Section 1.2), and the percentage of fine sand, silt, and clay in the bed material increases [4,41], particularly below RK 255 where the bed comprises Pleistocene and interdistributary clays [99]. Bank sediments, which control width, also become finer downstream, and the channel becomes less sinuous [99–102]. This scenario, along with the reduction in flow velocity, is conducive to an escalation in the strength of riverbanks and less capacity to incise the channel [22,103], permitting the development of narrower channel widths.

The decadal changes of pools and riffles in different times are also determined by comparing the elevation changes for the pools or riffles in the same location from three intervals (1952–1963, 1963–1992, and 1992–2013). The black lines in Figures 14 and 15 reference the scour (negative elevation change) and fill (positive elevation change). In detail, despite some scour that occurred from 1952–1963, the general pattern in both Figure 14A,B still demonstrate a net riverbed aggradation. Moreover, the patterns in 1963–1992 show slight degradation for both riffles and pools (Figure 14C,D). These results are consistent with the outcomes from cumulative elevation changes. The patterns of riffles (Figure 14C) can be well explained by the backwater effects, as net degradation occurred in downstream RK 270, while aggradation could be observed in upstream RK 270. The results from pools, on the contrary, have three positive peaks roughly ≥10 m, with the peak at RK 224 >20 m (Figure 14D). By neglecting these three peaks, the overall pattern shows net scour downstream of RK 203. In fact, prominent peaks are found in RK 224 from both Figure 14B (negative peak) and D (positive peak). If we exclude the 1963 elevation data in RK 224 (−59.5 m), and directly compare the values between 1952 (−40.3 m) and 1992 (−37.6 m), the outcome is more consistent with other results. Thus, it is possible that there was an error during the 1963 survey, and future studies should be aware of this possibility.

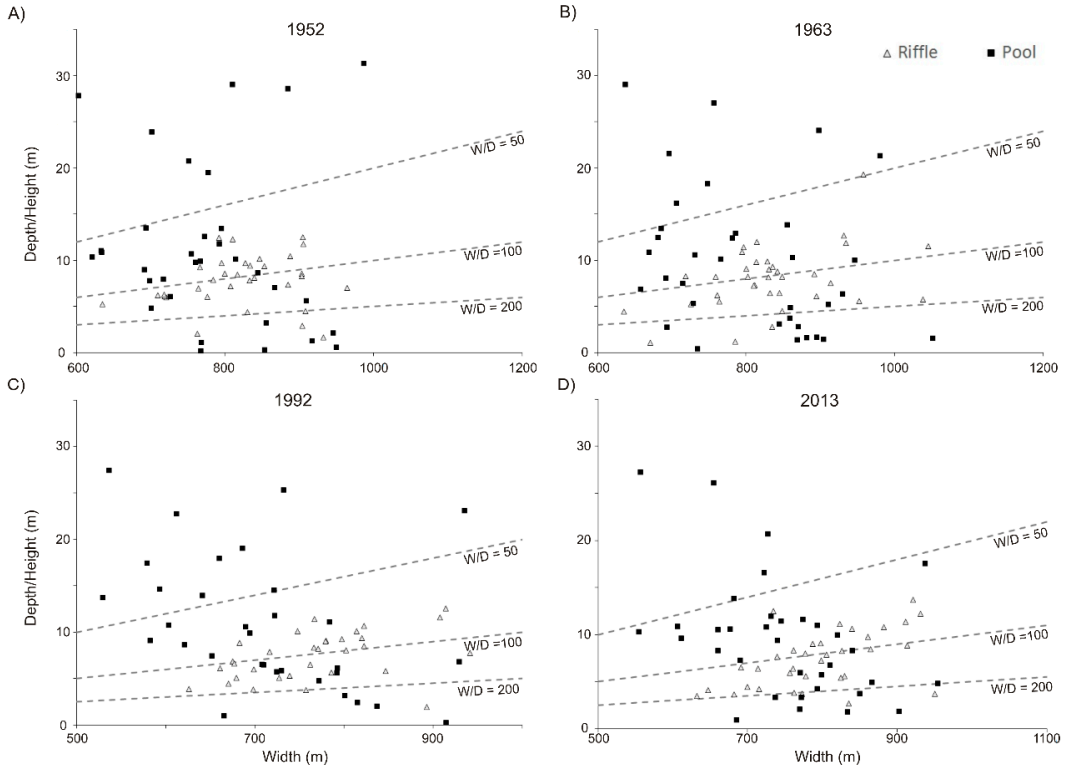

Figure 12. The depth vs. width for pools (solid squares) and the height vs. width for riffles (open triangles) in the upper reach at four different times: 1952 (**A**), 1963 (**B**), 1992 (**C**), and 2013 (**D**). Dashed lines represent constant width–depth ratios (W/D) of 50, 100, and 200. Note that the ranges of the *x*-axes in these four figures are slightly different.

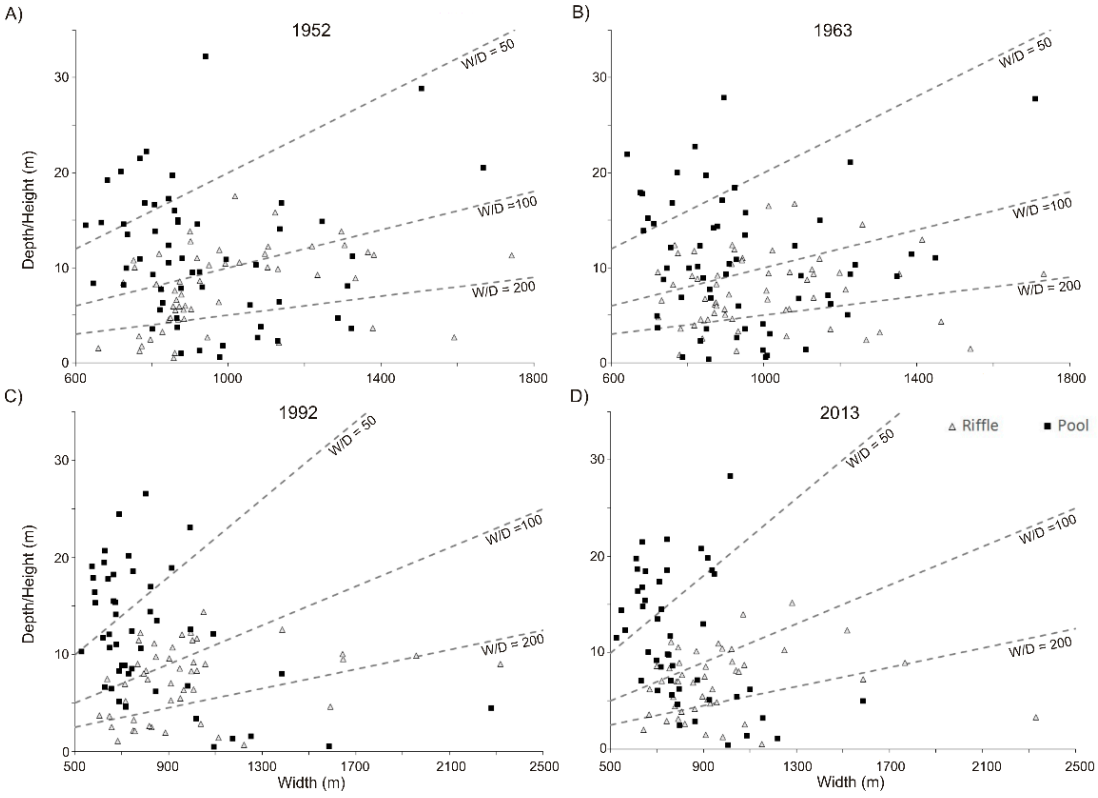

Figure 13. The W/D ratio for the lower reach at four different times: 1952 (**A**), 1963 (**B**), 1992 (**C**), and 2013 (**D**). All the descriptions are the same as Figure 12.

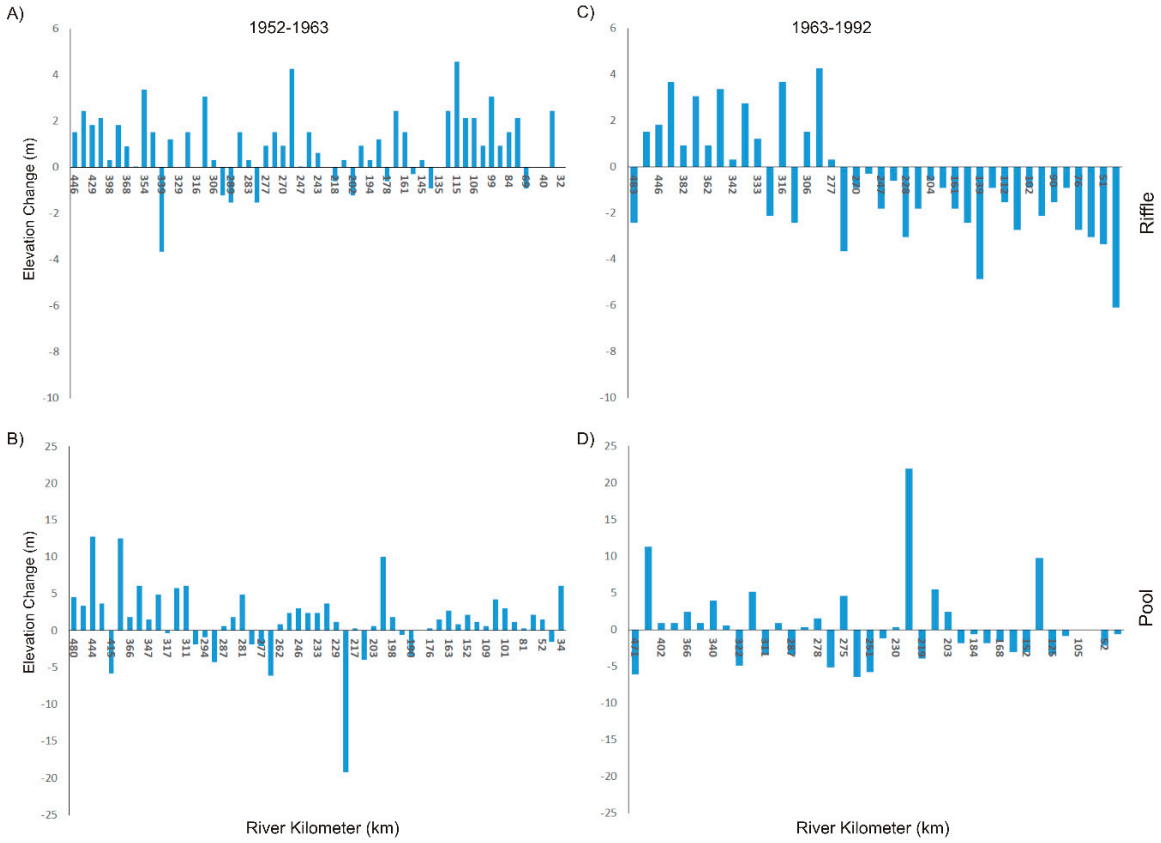

Figure 14. Elevation change of pools and riffles from 1952–1963 (**A** for riffles and **B** for pools) and 1963–1992 (**C** for riffles and **D** for pools). The decreases (<0) and increases (>0) are determined by reference to the *x*-axes at 0. We compared the differences in elevation for the same pools or riffles during these two time spans.

Figure 15 displays the elevation change of riffles and pools from 1992 to 2013 (i.e., between 1992–2004 and 2004–2013). Most of the results cluster between −6 and 6 m; only three peaks are either larger than 6 m (RK 471 and RK 34 in Figure 15A), or smaller than −6 m (RK 174 in Figure 15B). If we exclude these three peaks, the averaged values are both close to 0. Thus, by only examining Figure 15B, the riffle–pool sequences probably reach a stable status. In addition, Figure 15A,B were plotted by employing the sub-reaches divided by Wang and Xu [14], where these sub-reaches A–E were based on the different riverbed deformation trends. Their study concluded that reaches A and E experienced riverbed aggradation; in contrast, riverbed degradation occurred in reaches B and D (Figure 15). It is clear that the temporal elevation changes in riffles or pools between 1992 and 2013 are not identical to their findings. In addition, the entire riffle–pool pattern does not agree with the deposition or erosion patterns in these sub-reaches determined by Wang and Xu [14].

However, both of the trend lines from 1992–2004 and 2004–2013 in Figure 8 share an identical pattern to the riverbed deformation results from Wang and Xu [14]. Although the methods used in this study and by Wang and Xu [14] are different (their study generated riverbed profiles by averaging all the sounding points in a one-mile-long reach), the similar patterns suggest that the results from either thalweg change or averaging riverbed deformation can represent in-channel adjustments in the LMR. Therefore, given all the above mentioned findings, another possibility is that the disagreements between this study and that by Wang and Xu [14] regarding temporal changes of riffles or pools might be as a result of the vague definition of the riffle–pool sequence. Wang and Xu [14] did not indicate how they determined pool and riffles (i.e., tolerance value), whereas we used 6 m in this study. Therefore, the discrepancy of riffle–pool patterns between both studies is expected. In sum, temporal adjustments of riffles or pools are consistent with the thalweg deformation trends in this study. Furthermore, as the

patterns of the thalweg profiles and average riverbed deformation from Wang and Xu [14] are similar, the temporal variations regarding the entire LMR channel (i.e., thalweg, riffle–pool sequences, riverbed deformation) might be heavily controlled by similar factors, such as sediment supply or backwater effects. In addition, both the thalweg and averaged riverbed deformation can be proper indexes for the channel deformation.

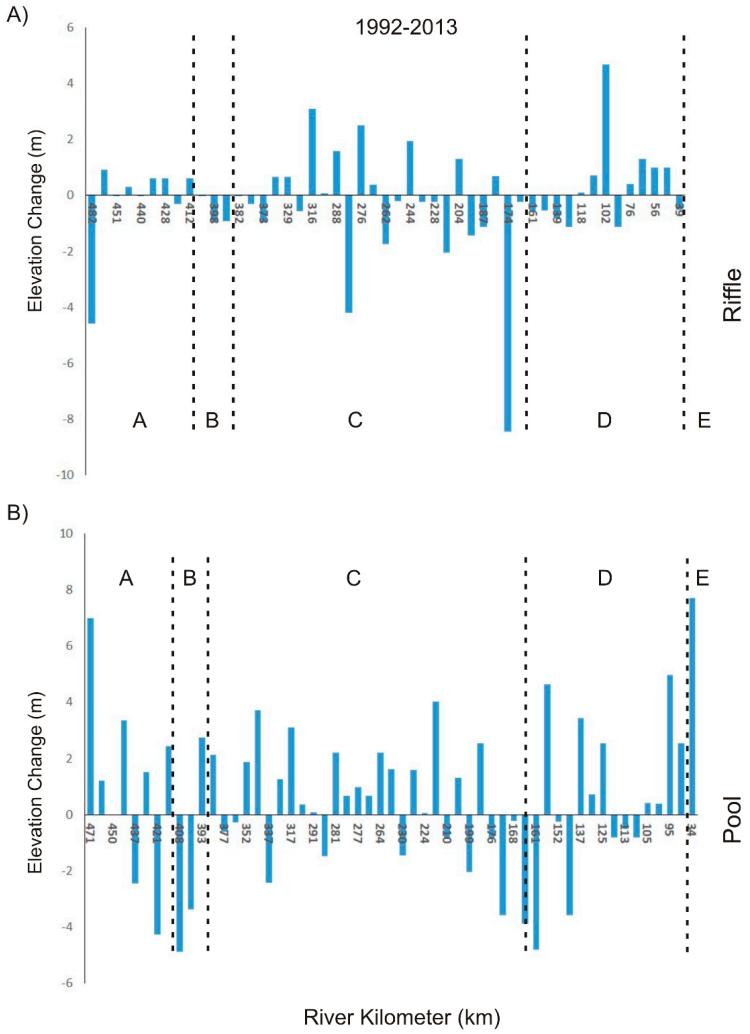

Figure 15. Similar to Figure 14, this figure delineates both scours and fills of riffles (**A**) and pools (**B**) from 1992–2013. The sub-reaches **A**–**E** are divided by adopting the concept from Wang and Xu [14]; different sub-reaches and their respective locations in RK are as follows: A = RK 500–412, B = RK 412–386, C = RK 386–163, D = RK 163–37, and E = RK 37–0.

5. Conclusions

An examination of hydrographic surveys from the mid-1950s to 2013 provided insights into morphological adjustment of the thalweg profiles, as well as the pool–riffle sequences in the LMR. This study covered the period from pre-construction to post-construction of the ORCS to scrutinize geomorphological response to the channel engineering, which is both time- and reach-dependent. By examining the thalweg elevation changes, the adjustments reveal a prominent variation in each period. The channel bed experienced aggradation along the entire LMR in pre-ORCS construction from 1952–1963. In addition, the results after 1975 (1975–1992 and 2004–2013) demonstrate a general trend of net degradation. The only exception occurred from 1992–2004, as the trend line shows that a net aggradation occurred within this period. The thalweg changes may be influenced by flood events, as both upstream aggradation and downstream degradation from 1963–1975 might have resulted from the

1973 flood. Net aggradation from 1992–2004 may be attributed to the input and deposition of sediments from upstream during the 1993 flood. In addition, due to the backwater effect, salt-water wedge, and the occasional flood-related diversion of flow and sediment near the BCS, the thalweg elevations substantially varied between the upper (RK 500 to RK 205) and the lower (RK 205 to RK 0) reaches.

Several findings of this study concern riffle–pool sequences. Firstly, the W_s results fall within the 5–7 ratio criteria, which is consistent with most previous studies. Secondly, the decrease of W/D ratios from the upper to the lower reaches reveals the decreasing ability to erode banks due to sediment cohesion in the lower reach. Thirdly, comparing temporal change in the same riffle or pool reveals that both scour and fill also follow a similar pattern as the cumulative elevation changes. The riverbed experienced aggradation from 1952–1963. After 1963 (from both 1963–1992 and 1992–2013), the trends show slight degradation, and eventually reach dynamic equilibrium. In addition, both patterns of the thalweg and averaged riverbed deformation [14] are extremely similar, which suggests that the in-channel deformation might be affected by similar factors, such as backwater effects. In addition, backwater effects might have impacted not only the bed elevation changes, but also the riffle pattern from 1963–1992.

In sum, our findings suggest that the LMR, the lower reach of one of world's largest river systems, experiences notable channel bed change due to flow regulation, as well as flood events. In the future, as global sea level keeps rising, it is believed that studies like these can benefit from understanding of morphodynamics in this large river system, and help in building strategies related to river management and engineering structures needed to protect the water and sediment resources of this low-lying deltaic area and its people.

Supplementary Materials: The following are available online at http://www.mdpi.com/2073-4441/11/6/1175/s1: Figure S1: Temporal trends of lengths and amplitude.

Author Contributions: C.-Y.W. performed most of the analyses, created most of the images and tables, and wrote the manuscript draft. J.M. developed the study concept, guided the analyses, created a few of the figures, and revised the manuscript. Both authors read and approved the final manuscript.

Funding: Publication of this article was funded in part by the University of Florida Open Access Publishing Fund.

Acknowledgments: The authors thank Paul F. Hudson from Leiden University, the Netherlands, for his suggestions, which further improved this manuscript. In addition, we would like to thank the two anonymous reviewers, as well as the guest editor Y. Jun Xu, who provided suggestions and comments.

Conflicts of Interest: The authors declare no conflicts of interest.

References

1. Schumm, S.A.; Rutherfurd, I.D. *Pre-Cutoff Morphology of the Lower Mississippi River*; The University of Melbourne: Parkville, Australia, 1994; pp. 13–44.
2. Milliman, J.D.; Farnsworth, K.L. *River Discharge to the Coastal Ocean: A global Synthesis*; Cambridge University Press: Cambridge, UK, 2013.
3. Fisk, H.N. *Geological Investigation of the Atchafalaya Basin and the Problem of Mississippi River Diversion*; Waterways Experiment Station: Vicksburg, MS, USA, 1952.
4. Mossa, J. Sediment dynamics in the lowermost Mississippi River. *Eng. Geol.* **1996**, *45*, 457–479. [CrossRef]
5. Kesel, R.H. The decline in the suspended load of the lower Mississippi River and its influence on adjacent wetlands. *Environ. Geol. Water Sci.* **1988**, *11*, 271–281. [CrossRef]
6. Kesel, R.H. Human modifications to the sediment regime of the Lower Mississippi River flood plain. *Geomorphology* **2003**, *56*, 325–334. [CrossRef]
7. Blum, M.D.; Roberts, H.H. Drowning of the Mississippi Delta due to insufficient sediment supply and global sea-level rise. *Nat. Geosci.* **2009**, *2*, 488. [CrossRef]
8. Blum, M.D.; Roberts, H.H. The Mississippi delta region: Past, present, and future. *Ann. Rev. Earth Planet. Sci.* **2012**, *40*, 655–683. [CrossRef]
9. Meade, R.H.; Moody, J.A. Causes for the decline of suspended-sediment discharge in the Mississippi River system, 1940–2007. *Hydrol. Process. Int. J.* **2010**, *24*, 35–49. [CrossRef]

10. Couvillion, B.R.; Barras, J.A.; Steyer, G.D.; Sleavin, W.; Fischer, M.; Beck, H.; Trahan, N.; Griffin, B.; Heckman, D. *Land Area Change in Coastal Louisiana from 1932 to 2010*; U.S. Geological Survey: Reston, AV, USA, 2011.
11. Nittrouer, J.A.; Allison, M.A.; Campanella, R. Bedform transport rates for the lowermost Mississippi River. *J. Geophys. Res. Earth Surf.* **2008**, *113*. [CrossRef]
12. Rosen, T.; Xu, Y. A hydrograph-based sediment availability assessment: Implications for Mississippi River sediment diversion. *Water* **2014**, *6*, 564–583. [CrossRef]
13. Rosen, T.; Xu, Y.J. Estimation of sedimentation rates in the distributary basin of the Mississippi River, the Atchafalaya River Basin, USA. *Hydrol. Res.* **2013**, *46*, 244–257. [CrossRef]
14. Wang, B.; Xu, Y.J. Decadal-Scale Riverbed Deformation and Sand Budget of the Last 500 km of the Mississippi River: Insights into Natural and River Engineering Effects on a Large Alluvial River. *J. Geophys. Res. Earth Surf.* **2018**, *123*, 874–890. [CrossRef]
15. Joshi, S.; Xu, Y.J. Assessment of Suspended Sand Availability under Different Flow Conditions of the Lowermost Mississippi River at Tarbert Landing during 1973–2013. *Water* **2015**, *7*, 7022–7044. [CrossRef]
16. Joshi, S.; Xu, Y.J. Bedload and Suspended Load Transport in the 140-km Reach Downstream of the Mississippi River Avulsion to the Atchafalaya River. *Water* **2017**, *9*, 716. [CrossRef]
17. Wang, B.; Xu, Y.J. Bedload Transport at the Mississippi-Atchafalaya River Diversion. *Coast. Sediments* **2019**, 2930–2943. [CrossRef]
18. Curran, J.H.; Wohl, E.E. Large woody debris and flow resistance in step-pool channels, Cascade Range, Washington. *Geomorphology* **2003**, *51*, 141–157. [CrossRef]
19. Harmar, O.P.; Clifford, N.J.; Thorne, C.R.; Biedenharn, D.S. Morphological changes of the Lower Mississippi River: Geomorphological response to engineering intervention. *River Res. Appl.* **2005**, *21*, 1107–1131. [CrossRef]
20. Harmar, O.P.; Clifford, N.J. Geomorphological explanation of the long profile of the Lower Mississippi River. *Geomorphology* **2007**, *84*, 222–240. [CrossRef]
21. Knighton, D. *Fluvial Forms and Processes: A New Perspective*; Routledge: Abingdon, UK, 2014.
22. Hudson, P. Pool-Riffle Morphology in an Actively Migrating Alluvial Channel: The Lower Mississippi River. *Phys. Geogr.* **2002**, *23*, 154–169. [CrossRef]
23. Leopold, L.B.; Wolman, M.G.; Miller, J.P. *Fluvial Processes in Geomorphology*; Courier Corporation: Chelmsford, MA, USA, 2012.
24. Montgomery, D.R.; Buffington, J.M. Channel-reach morphology in mountain drainage basins. *Geol. Soc. Am. Bull.* **1997**, *109*, 596–611. [CrossRef]
25. Nelson, P.A.; Brew, A.K.; Morgan, J.A. Morphodynamic response of a variable-width channel to changes in sediment supply. *Water Resour. Res.* **2015**, *51*, 5717–5734. [CrossRef]
26. Leopold, L.B.; Wolman, M.G. River meanders. *Geol. Soc. Am. Bull.* **1960**, *71*, 769–793. [CrossRef]
27. Keller, E.A.; Melhorn, W.N. Rhythmic spacing and origin of pools and riffles. *Geol. Soc. Am. Bull.* **1978**, *89*, 723–730. [CrossRef]
28. Richards, K.S. Channel width and the riffle-pool sequence. *Geol. Soc. Am. Bull.* **1976**, *87*, 883–890. [CrossRef]
29. Richards, K.S. The morphology of riffle-pool sequences. *Earth Surf. Process.* **1976**, *1*, 71–88. [CrossRef]
30. Clifford, N.J. Formation of riffle—Pool sequences: Field evidence for an autogenetic process. *Sediment. Geol.* **1993**, *85*, 39–51. [CrossRef]
31. Calderon, M.S.; An, K.-G. An influence of mesohabitat structures (pool, riffle, and run) and land-use pattern on the index of biological integrity in the Geum River watershed. *J. Ecol. Environ.* **2016**, *40*, 13. [CrossRef]
32. Jowett, I.G. A method for objectively identifying pool, run, and riffle habitats from physical measurements. *N. Z. J. Mar. Freshw. Res.* **1993**, *27*, 241–248. [CrossRef]
33. Keller, E.A. Pools, riffles, and channelization. *Environ. Geol.* **1978**, *2*, 119–127. [CrossRef]
34. Joshi, S.; Jun, X.Y. Recent changes in channel morphology of a highly engineered alluvial river—The Lower Mississippi River. *Phys. Geogr.* **2018**, *39*, 140–165. [CrossRef]
35. Milliman, J.D.; Meade, R.H. World-wide delivery of river sediment to the oceans. *J. Geol.* **1983**, *91*, 1–21. [CrossRef]
36. Meade, R.H. River-sediment inputs to major deltas. In *Sea-Level Rise and Coastal Subsidence*; Springer: Berlin, Germany, 1996; pp. 63–85.

37. Nittrouer, J.A.; Shaw, J.; Lamb, M.P.; Mohrig, D. Spatial and temporal trends for water-flow velocity and bed-material sediment transport in the lower Mississippi River. *Geol. Soc. Am. Bull.* **2012**, *124*, 400–414. [CrossRef]
38. Allison, M.A.; Demas, C.R.; Ebersole, B.A.; Kleiss, B.A.; Little, C.D.; Meselhe, E.A.; Powell, N.J.; Pratt, T.C.; Vosburg, B.M. A water and sediment budget for the lower Mississippi–Atchafalaya River in flood years 2008–2010: Implications for sediment discharge to the oceans and coastal restoration in Louisiana. *J. Hydrol.* **2012**, *432*, 84–97. [CrossRef]
39. Benke, A.C.; Cushing, C.E. *Rivers of North America*; Elsevier: Amsterdam, The Netherlands, 2011.
40. Nittrouer, J.A.; Mohrig, D.; Allison, M.A.; PEYRET, A.-P.B. The lowermost Mississippi River: A mixed bedrock-alluvial channel. *Sedimentology* **2011**, *58*, 1914–1934. [CrossRef]
41. Keown, M.P.; Dardeau, E.A., Jr.; Causey, E.M. Historic Trends in the Sediment Flow Regime of the Mississippi River. *Water Resour. Res.* **1986**, *22*, 1555–1564. [CrossRef]
42. Nittrouer, J.A.; Mohrig, D.; Allison, M. Punctuated sand transport in the lowermost Mississippi River. *J. Geophys. Res. Earth Surf.* **2011**, *116*, F04025. [CrossRef]
43. Seed, R.B.; Bea, R.G.; Abdelmalak, R.I.; Athanasopoulos, A.G.; Boutwell, G.P., Jr.; Bray, J.D.; Briaud, J.-L.; Cheung, C.; Cobos-Roa, D.; Cohen-Waeber, J. *Investigation of the Performance of the New Orleans Flood Protection System in Hurricane Katrina on August 29, 2005: Volume 2*; Independent Levee Investigation Team: New Orleans, MS, USA, 2006; Volume 2.
44. Elliott, D.O. *Improvement of the Lower Mississippi River for Flood Control and Navigation*; MRC Print: Louis, MO, USA, 1932.
45. Ferguson, H.B. *History of the Improvement of the Lower Mississippi River for Flood Control and Navigation, 1932–1939*; MRC Print: Louis, MO, USA, 1940.
46. Moore, N.R. *Improvement of the Lower Mississippi River and Tributaries, 1931–1972*; Mississippi River Commission: Vicksburg, MS, USA, 1972.
47. Mossa, J.; Chen, Y.-H.; Wu, C.-Y. Geovisualization geoscience of large river floodplains. *J. Maps* **2019**, 1–17. [CrossRef]
48. Copeland, R.R.; Thomas, W.A. *Lower Mississippi River Tarbert Landing to East Jetty Sedimentation Study*; Numerical Model Investigation; Army Engineer Waterways Experiment Station: Vicksburg, MS, USA, 1992.
49. Mossa, J. Historical changes of a major juncture: Lower Old River, Louisiana. *Phys. Geogr.* **2013**, *34*, 315–334. [CrossRef]
50. Biedenharn, D.S.; Thorne, C.R.; Watson, C.C. Recent morphological evolution of the Lower Mississippi River. *Geomorphology* **2000**, *34*, 227–249. [CrossRef]
51. Yang, C.T. Formation of Riffles and Pools. *Water Resour. Res.* **1971**, *7*, 1567–1574. [CrossRef]
52. Clifford, N.J.; Richards, K.S. The reversal hypothesis and the maintenance of riffle-pool sequences: A review and field appraisal. In *Lowland Floodplain Rivers: Geomorphological Perspectives*; Carling, P., Petts, G.E., Eds.; John Wiley: Chichester, UK, 1992; pp. 43–70.
53. Keller, E.A. Development of alluvial stream channels: A five-stage model. *Geol. Soc. Am. Bull.* **1972**, *83*, 1531–1536. [CrossRef]
54. Lisle, T. A sorting mechanism for a riffle-pool sequence. *Geol. Soc. Am. Bull.* **1979**, *90*, 1142–1157. [CrossRef]
55. Sear, D.A. Sediment transport processes in pool-riffle sequences. *Earth Surf. Process. Landf.* **1996**, *21*, 241–262. [CrossRef]
56. Milan, D.J.; Heritage, G.L.; Large, A.R.G.; Charlton, M.E. Stage dependent variability in tractive force distribution through a riffle–pool sequence. *Catena* **2001**, *44*, 85–109. [CrossRef]
57. Clifford, N.J. Differential bed sedimentology and the maintenance of riffle-pool sequences. *Catena* **1993**, *20*, 447–468. [CrossRef]
58. Thompson, D.M.; Wohl, E.E.; Jarrett, R.D. Velocity reversals and sediment sorting in pools and riffles controlled by channel constrictions. *Geomorphology* **1999**, *27*, 229–241. [CrossRef]
59. Milan, D.J.; Heritage, G.L.; Large, A.R.G. Tracer pebble entrainment and deposition loci: Influence of flow character and implications for riffle-pool maintenance. *Geol. Soc. Lond. Spec. Publ.* **2002**, *191*, 133–148. [CrossRef]
60. Thompson, D.M. Random controls on semi-rhythmic spacing of pools and riffles in constriction-dominated rivers. *Earth Surf. Process. Landf.* **2001**, *26*, 1195–1212. [CrossRef]
61. Leopold, A.C. *Plant Growth and Development*; Mcgraw-Hill Book Company: New York, NY, USA, 1964.

62. Bovee, K.D.; Milhous, R. *Hydraulic Simulation in Instream Flow Studies: Theory and Techniques*; IFIP No. 5; US Fish and Wildlife Service: Washington, DC, USA, 1978.
63. Hey, R.D.; Thorne, C.R. Stable channels with mobile gravel beds. *J. Hydraul. Eng.* **1986**, *112*, 671–689. [CrossRef]
64. Slocombe, M.L.; Davis, J.D. Morphology of small, discontinuous montane meadow streams in the Sierra Nevada. *Geomorphology* **2014**, *219*, 103–113. [CrossRef]
65. Gibson, S.; Osorio, A.; Creech, C.; Amorim, R.; Dircksen, M.; Dahl, T.; Koohafkan, M. Two pool-to-pool spacing periods on large sand-bed rivers: Mega-pools on the Madeira and Mississippi. *Geomorphology* **2019**, *328*, 196–210. [CrossRef]
66. Montgomery, D.R.; Buffington, J.M.; Smith, R.D.; Schmidt, K.M.; Pess, G. Pool spacing in forest channels. *Water Resour. Res.* **1995**, *31*, 1097–1105. [CrossRef]
67. Wohl, E.E.; Vincent, K.R.; Merritts, D.J. Pool and riffle characteristics in relation to channel gradient. *Geomorphology* **1993**, *6*, 99–110. [CrossRef]
68. Dury, G.H. A Re-Survey of Part of the Hawkesbury River, New South Wales, After One Hundred Years. *Geogr. Res.* **1970**, *8*, 121–132. [CrossRef]
69. Hudson, P.F.; Kesel, R.H. Spatial and temporal adjustment of the lower Mississippi River to major human impacts. *Z. Geomorphol. Suppl.* **2006**, *143*, 17–33.
70. Allison, M.A.; Meselhe, E.A. The use of large water and sediment diversions in the lower Mississippi River (Louisiana) for coastal restoration. *J. Hydrol.* **2010**, *387*, 346–360. [CrossRef]
71. Smith, L.M.; Winkley, B.R. The response of the Lower Mississippi River to river engineering. *Eng. Geol.* **1996**, *45*, 433–455. [CrossRef]
72. Biedenharn, D.S.; Watson, C.C. Stage adjustment in the lower Mississippi River, USA. *Regul. Rivers Res. Manag.* **1997**, *13*, 517–536. [CrossRef]
73. Meselhe, E.A.; Sadid, K.M.; Allison, M.A. Riverside morphological response to pulsed sediment diversions. *Geomorphology* **2016**, *270*, 184–202. [CrossRef]
74. Wang, B.; Xu, Y.J. Long-term geomorphic response to flow regulation in a 10-km reach downstream of the Mississippi–Atchafalaya River diversion. *J. Hydrol. Reg. Stud.* **2016**, *8*, 10–25. [CrossRef]
75. Ramirez, M.T.; Allison, M.A. Suspension of bed material over sand bars in the Lower Mississippi River and its implications for Mississippi delta environmental restoration. *J. Geophys. Res. Earth Surf.* **2013**, *118*, 1085–1104. [CrossRef]
76. Wang, B.; Xu, Y. Sediment trapping by emerged channel bars in the lowermost Mississippi River during a major flood. *Water* **2015**, *7*, 6079–6096. [CrossRef]
77. Kesel, R.H.; Yodis, E.G.; McCraw, D.J. An approximation of the sediment budget of the lower Mississippi River prior to major human modification. *Earth Surf. Process. Landf.* **1992**, *17*, 711–722. [CrossRef]
78. Wu, C.-Y.; Mossa, J.; Mao, L.; Almulla, M. Comparison of different spatial interpolation methods for historical hydrographic data of the lowermost Mississippi River. *Ann. GIS* **2019**, *0*, 1–19. [CrossRef]
79. Welch, R.; Homsey, A. Datum Shifts for UTM Coordinates. *Photogramm. Eng. Remote Sens.* **1997**, *63*, 371–375.
80. Carling, P.A.; Orr, H.G. Morphology of riffle–pool sequences in the River Severn, England. *Earth Surf. Process. Landf.* **2000**, *25*, 369–384. [CrossRef]
81. O'Neill, M.P.; Abrahams, A.D. Objective identification of pools and riffles. *Water Resour. Res.* **1984**, *20*, 921–926. [CrossRef]
82. Lofthouse, C.; Robert, A. Riffle–pool sequences and meander morphology. *Geomorphology* **2008**, *99*, 214–223. [CrossRef]
83. Harmar, O.P. Morphological and Process Dynamics of the Lower Mississippi River. Ph.D. Thesis, University of Nottingham, Nottingham, UK, 2004.
84. Milne, J.A. Bed-material size and the riffle-pool sequence. *Sedimentology* **1982**, *29*, 267–278. [CrossRef]
85. Knox, R.L.; Latrubesse, E.M. A geomorphic approach to the analysis of bedload and bed morphology of the Lower Mississippi River near the Old River Control Structure. *Geomorphology* **2016**, *268*, 35–47. [CrossRef]
86. Kesel, R.H.; Dunne, K.C.; McDonald, R.C.; Allison, K.R.; Spicer, B.E. Lateral erosion and overbank deposition on the Mississippi River in Louisiana caused by 1973 flooding. *Geology* **1974**, *2*, 461–464. [CrossRef]
87. Chatanantavet, P.; Lamb, M.P.; Nittrouer, J.A. Backwater controls of avulsion location on deltas. *Geophys. Res. Lett.* **2012**, *39*. [CrossRef]

88. Mossa, J. The changing geomorphology of the Atchafalaya River, Louisiana: A historical perspective. *Geomorphology* **2016**, *252*, 112–127. [CrossRef]
89. Day, J.; Hunter, R.; Keim, R.F.; DeLaune, R.; Shaffer, G.; Evers, E.; Reed, D.; Brantley, C.; Kemp, P.; Day, J. Ecological response of forested wetlands with and without large-scale Mississippi River input: Implications for management. *Ecol. Eng.* **2012**, *46*, 57–67. [CrossRef]
90. Lamb, M.P.; Nittrouer, J.A.; Mohrig, D.; Shaw, J. Backwater and river plume controls on scour upstream of river mouths: Implications for fluvio-deltaic morphodynamics. *J. Geophys. Res. Earth Surf.* **2012**, *117*, F01002. [CrossRef]
91. Lane, E.W. *A Study of the Shape of Channels formed by Natural Streams Flowing in Erodible Material*; US Army Corps of Engineers: Omaha, NE, USA, 1957.
92. Chow, V.T. *Open-Channel Hydraulics*; McGraw-Hill: New York, NY, USA, 1959; Volume 1.
93. Fagerburg, T.L.; Alexander, M.P. *Underwater Sill Construction for Mitigating Salt Wedge Migration on the Lower Mississippi River*; Army Engineer Waterways Experiment Station: Vicksburg, MS, USA, 1994.
94. McAnally, W.H.; Pritchard, D.W. Salinity control in Mississippi River under drought flows. *J. Waterw. Port Coast. Ocean Eng.* **1997**, *123*, 34–40. [CrossRef]
95. Saucier, R.T. *Geomorphology and Quarternary Geologic History of the Lower Mississippi Valley*; Army Engineer Waterways Experiment Station: Vicksburg, MS, USA, 1994; Volume 2.
96. Galler, J.J.; Allison, M.A. Estuarine controls on fine-grained sediment storage in the Lower Mississippi and Atchafalaya Rivers. *Geol. Soc. Am. Bull.* **2008**, *120*, 386–398. [CrossRef]
97. Chin, E.H.; Skelton, J.; Guy, H.P. The 1973 Mississippi River basin flood; compilation and analyses of meteorologic, streamflow, and sediment data. *US Govt. Print. Off.* **1975**, *937*. [CrossRef]
98. Schumm, S.A. The effect of sediment type on the shape and stratification of some modern fluvial deposits. *Am. J. Sci.* **1960**, *258*, 177–184. [CrossRef]
99. Kolb, C.R. Sediments forming the bed and banks of the lower Mississippi River and their effect on river migration. *Sedimentology* **1963**, *2*, 227–234. [CrossRef]
100. Krinitzsky, E.L. *Geological Influences on Bank Erosion along Meanders of the Lower Mississippi River*; Army Engineer Waterways Experiment Station: Vicksburg, MS, USA, 1965.
101. Schumm, S.A.; Spitz, W.J. Geological influences on the Lower Mississippi River and its alluvial valley. *Eng. Geol.* **1996**, *45*, 245–261. [CrossRef]
102. Edmonds, D.A.; Slingerland, R.L. Significant effect of sediment cohesion on delta morphology. *Nat. Geosci.* **2009**, *3*, 105. [CrossRef]
103. Knighton River Channel Adjustment—The Downstream Dimension. In *River Channels: Environment and Process*; Blackwell: Oxford, UK, 1987; pp. 95–128.